

Asymmetric spin crossover behaviour and evidence of light-induced excited spin state trapping in a dinuclear iron(II) helicate†

Diane Pelleteret,^a Rodolphe Clérac,^{*cd} Corine Mathonière,^{ef} Etienne Harté,^{cd} Wolfgang Schmitt^{*a} and Paul E. Kruger^{*ab}

Received (in Cambridge, UK) 16th September 2008, Accepted 7th November 2008

First published as an Advance Article on the web 19th November 2008

DOI: 10.1039/b816196h

Reported herein are the synthesis, structural and magnetic characterisation of a dinuclear Fe^{II} triple helicate that displays an unprecedented reversible asymmetric high spin to low spin crossover characterised by a thermal hysteresis: indeed the high spin state can be recovered by white light irradiation at 10 K.

Currently there is an ever increasing interest in spin crossover compounds, partly motivated by their potential application as molecular memory or visual display devices,¹ which has led to a better understanding of the parameters (temperature, pressure, light, structure *etc.*) that influence this fascinating phenomenon.² Spin crossover is best exemplified by the low spin Fe^{II} ($S = 0$) to high spin Fe^{II} ($S = 2$) conversion. Nevertheless, scant literature deals with dinuclear Fe^{II} spin crossover helicate complexes. In this respect, Williams reported a dinuclear Fe^{II} helicate with thermally induced two-step spin crossover with negative cooperativity,³ whereas Tuna synthesised a series of Fe^{II} helicate species using a variety of counter anions that exhibited various spin crossover behaviours, which were later reinterpreted by Gütllich.^{4,5} More recently, Kojima reported two Fe^{II} helicate compounds presenting either no magnetic conversion or an abrupt [LS–HS] to [HS–HS] spin crossover (LS and HS stand for low spin and high spin, respectively).⁶

The synthesis and characterisation of helicate species has been closely associated with the development of metallo-supramolecular chemistry.⁷ Recently we reported using metallohelicate complexes as molecular hosts and monitored anion binding within their intra-helical cavities through ¹H NMR spectroscopy.⁸ Indeed, the inclusion of spin crossover

within an Fe^{II} metallohelicate complex makes them very attractive targets for the recognition of guest molecules using the spin crossover magnetic signature.

With the motivation of using metallohelicates in the formation of supramolecular devices, we have commenced a study into the nature of the spin crossover in dinuclear Fe^{II} helicate complexes and its dependence on the structure and functionality of the ligand. We wish to explore the possibility of generating one-step [HS–HS] to [LS–LS] spin crossover helicates since we believe that the larger associated structural and electronic changes are of advantage for device or sensor application. To this end we synthesised the new bis-bidentate ligand **L** which contains imidazolinine ‘head groups’ (to access spin crossover behaviour) linked *via* a conjugated and rigid oxydianiline bridge (to generate a helicate). The corresponding triple-stranded Fe^{II} helicate [Fe₂(L)₃](ClO₄)₄, **1**, was synthesised and its ability to undergo a spin crossover upon temperature variation and light irradiation was studied by both magnetic susceptibility and reflectivity measurements.

The bis-bidentate ligand **L** was synthesised by Schiff-base condensation in methanol using two equivalents of 1-methyl-2-imidazolecarboxaldehyde and one equivalent of 4,4'-oxydianiline. The corresponding Fe^{II} dinuclear helicate, **1**, was obtained in good yield by stirring three equivalents of **L** with two equivalents of Fe(ClO₄)₂·6H₂O in methanol for 30 minutes.† The expected triple-stranded helical structure was highlighted by ¹H NMR spectroscopy and confirmed by single crystal X-ray diffraction‡ for 1·2MeCN, Fig. 1. As anticipated, the structure of 1·2MeCN consists of a dinuclear triple helicate within which the Fe^{II} centres are in pseudo-octahedral environments bound to three imidazolinine units from three different ligands. Each ligand binds to two Fe^{II} centres, yielding an intra-helical metal–metal separation of 11.35 Å.

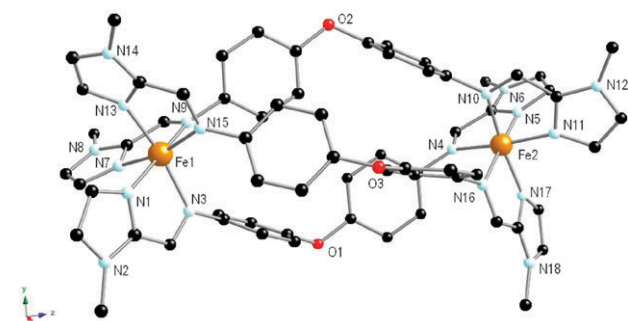


Fig. 1 Molecular structure of the triple helicate [Fe₂(L)₃]⁴⁺, **1**, at 150 K. Hydrogen atoms, perchlorate anions and MeCN solvate molecules are omitted for clarity.

^a University of Dublin, Trinity College, School of Chemistry, Dublin 2, Ireland. E-mail: paul.kruger@tcd.ie. E-mail: schmittw@tcd.ie

^b Department of Chemistry, University of Canterbury, Private Bag 4800, Christchurch, 8041, New Zealand.

E-mail: paul.kruger@canterbury.ac.nz

^c CNRS, UPR 8641, Centre de Recherche Paul Pascal (CRPP), Equipe ‘Matériaux Moléculaires Magnétiques’, 115 avenue du Dr. Albert Schweitzer, Pessac, F-33600, France.

E-mail: clerac@crpp-bordeaux.cnrs.fr

^d Université de Bordeaux, UPR 8641, Pessac, F-33600, France

^e CNRS, UPR 9048, Institut de Chimie de la Matière Condensée de Bordeaux (ICMCB), 87 avenue du Dr. Albert Schweitzer, Pessac, F-33608, France

^f Université de Bordeaux, UPR 9048, Pessac, F-33608, France

† Electronic supplementary information (ESI) available: Experimental details, selected distances and angles for 1·2MeCN, NMR data, TGA data, optical density spectrum for **1**, supplementary surface absorption spectra for **1**, additional magnetic and photomagnetic data. CCDC 702672. For ESI and crystallographic data in CIF or other electronic format see DOI: 10.1039/b816196h

Table 1 Selected bond lengths [Å] and bite angles [°] for **1**·2MeCN

		Fe–N _{imidazole} [Å]		Fe–N _{imine} [Å]	Bite angle [°]
Fe1	N1	1.976(3)	N3	2.028(3)	80.19(11)
	N7	1.959(3)	N9	2.004(3)	80.41(11)
	N13	1.967(3)	N15	2.042(3)	80.02(11)
Fe2	N5	1.965(3)	N4	2.027(3)	79.53(11)
	N11	1.960(3)	N10	2.026(3)	79.90(12)
	N17	1.975(3)	N16	2.009(3)	80.35(12)

Four of the six aryl rings in the centre of the helicate participate in interstrand edge-to-face CH $\cdots\pi$ bonding which support the helical structure. However, there are no significant intermolecular contacts of any nature between adjacent helicates. The similarity observed for the Fe–N bond distances and bite angles around Fe1 and Fe2 illustrates that at 150 K, both metal centres are in the low spin configuration, Table 1. Therefore the magnetic properties of this helicate system have been studied as a function of temperature to probe the possibility of spin crossover behaviour.

At 300 K, the value observed for the χT product (6.6 cm³ K mol^{−1}) is in good agreement with the presence of two $S = 2$ high spin Fe^{II} metal ions ($C = 3.3$ cm³ K mol^{−1} with $g = 2.1$). When the temperature is lowered, the χT product is almost constant down to 250 K and then decreases with a typical S-shape curve observed for spin crossover systems, Fig. 2. At 80 K, the spin crossover behavior is completed and a residual paramagnetic signal (at 40 K: 0.35 cm³ K mol^{−1}) is observed, most likely coming from residual HS Fe^{II} sites induced by structural or topological defects.² As shown in Fig. 2, a small thermal hysteresis effect is observed suggesting a structural phase transition associated with the spin crossover process. The first derivative of the χT product relative to the temperature, $d\chi T/dT$, in cooling mode leaves no ambiguity regarding the nature of the spin crossover process occurring in one [HS–HS] \leftrightarrow [LS–LS] step at $T_{1/2} = 140$ K. Nevertheless in the heating mode, the result is reproducibly different suggesting that the Fe^{II} sites switch successively in a two-step process within a narrow temperature range of 147–166 K.

Next, solid-state reflectivity spectra were collected on **1** under white light irradiation between 280 and 10 K, Fig. 3 top.† On decreasing temperature from 280 K to 100 K, the absorption at ca. 818 nm, assigned to the $d-d$ transition of the HS Fe^{II} ions in an octahedral environment $^5T_2 \rightarrow ^5E$, disappears while a new absorption band at ca. 630 nm, assigned to the MLCT of the Fe^{II} ions in a LS state, appears. If the temperature is lowered

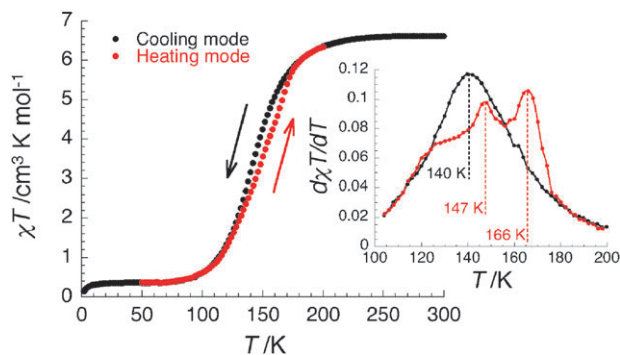


Fig. 2 χT versus T plot for **1** at 1000 Oe with χ being the magnetic susceptibility equal to M/H normalized by dinuclear helicate (temperature sweep rate 0.6 K/min). Inset: $d\chi T/dT$ versus T plot.

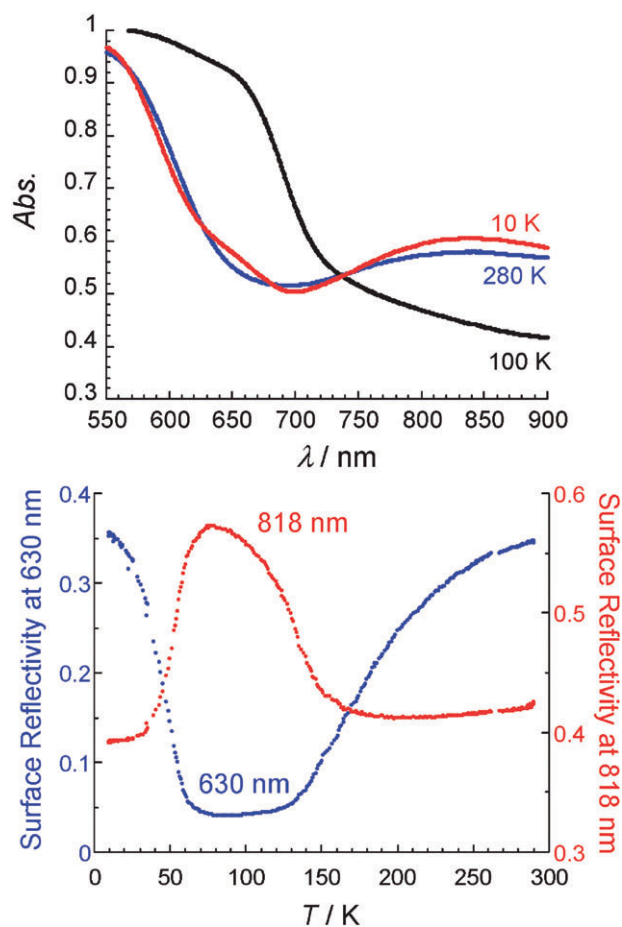


Fig. 3 Selected surface absorption spectra of **1** at different temperatures (top), and temperature dependence of surface reflectivity of **1** at 818 and 630 nm (bottom). All data between 280 and 10 K were collected at a cooling rate of 3 K/min.

further from 100 K to 10 K, the reverse process is observed suggesting a light induced phenomenon. The band at ca. 818 nm regains almost its original intensity while the band at ca. 630 nm disappears. As a result, the spectra obtained at 280 K and 10 K are almost identical. The concomitance of the optical changes observed upon cooling under white light irradiation is highlighted by the plot of the surface reflectivity at 818 and 630 nm as a function of temperature, Fig. 3, bottom. To interpret these data, it is interesting to compare them with the magnetic data obtained in the dark. The thermal dependence of the optical spectra between 280–100 K is related to the thermal dependence of the χT product and the spin crossover phenomenon. At 280 K, **1** is totally in a [HS–HS] state with a characteristic absorption at ca. 818 nm; and at 100 K, **1** is in a [LS–LS] state with a characteristic absorption at ca. 630 nm. Below 60 K, and under white light irradiation, the compound recovers its 280 K spectral feature (*i.e.* colour), suggesting strongly that the [LS–LS] state can be photoexcited. Therefore we have probed the possibility to recover the [HS–HS] phase from the [LS–LS] phase at low temperature using continuous light irradiation.

As suggested by the optical data, a light-induced excited spin state trapping (LIESST) effect is clearly observed when red (650 nm) or white light (clearly more efficient) irradiation is applied on **1** for example at 10 K, Fig. 4 inset. The χT product at

10 K has an initial value of $0.35 \text{ cm}^3 \text{ K mol}^{-1}$ and increases rapidly to a close saturation regime at $6 \text{ cm}^3 \text{ K mol}^{-1}$ after only 1.1 hours under white light irradiation, Fig. 4 inset. When the irradiation was stopped, the χT of the photoproduct was measured as a function of temperature between 2–300 K, Fig. 4. First of all, the increase of the χT product from $2.0 \text{ cm}^3 \text{ K mol}^{-1}$ at 2 K up to $6.4 \text{ cm}^3 \text{ K mol}^{-1}$ at 30 K (Fig. 4, point 1), is likely to be the signature of the magnetic anisotropy of the HS Fe^{II} ions as seen previously for other spin crossover Fe^{II} systems but may also be related to weak antiferro-magnetic interactions between HS Fe^{II} sites within the dinuclear complex.⁹ It is worth noting that the value of $6.4 \text{ cm}^3 \text{ K mol}^{-1}$ obtained at 30 K is very close to the value for the [HS–HS] phase obtained at 300 K ($6.6 \text{ cm}^3 \text{ K mol}^{-1}$) and indicates a quasi-quantitative photoconversion of the [LS–LS] state to the [HS–HS] state. Increasing the temperature at a sweep rate of about 0.6 K min^{-1} , the light induced [HS–HS] phase relaxes with a complicated sequence of regimes. A first relaxation of the metastable [HS–HS] state is observed around 50 K with an abrupt drop of the χT product down to about half of the 30 K value ($3.2 \text{ cm}^3 \text{ K mol}^{-1}$ at 50 K, Fig. 4, point 2), then a second slower regime of relaxation is observed up to 80 K (Fig. 4, point 3). Even if it is difficult to speculate on the origin of this two-step relaxation process without structural data after irradiation, this behavior strongly suggests the presence of two different relaxation mechanisms (and thus relaxation times) associated with the two Fe^{II} sites of the dinuclear complex: *i.e.* one HS Fe^{II} site seems to relax faster than the second one of the same dinuclear unit generating [LS–HS] species. Upon increasing temperature, the relaxation process of the photo-induced [HS–HS] state to [LS–LS] and [LS–HS] states is in competition with the thermal spin crossover that favors the appearance of HS Fe^{II} . Therefore at 80 K, the system is probably heterogeneous with [LS–LS] species and still a few metastable [LS–HS] species (Fig. 4, point 3). A first thermally induced spin crossover step between 80 and 110 K (Fig. 4, point 4) seems to convert some of the LS Fe^{II} sites into HS Fe^{II} . This first thermally induced spin crossover process occurs clearly at a lower temperature than the spin crossover observed around 140 K in Fig. 2. This result suggests that the present behavior might be the signature of the non-thermodynamic dinuclear [LS–HS] species that are thermally converted into [HS–HS] units.

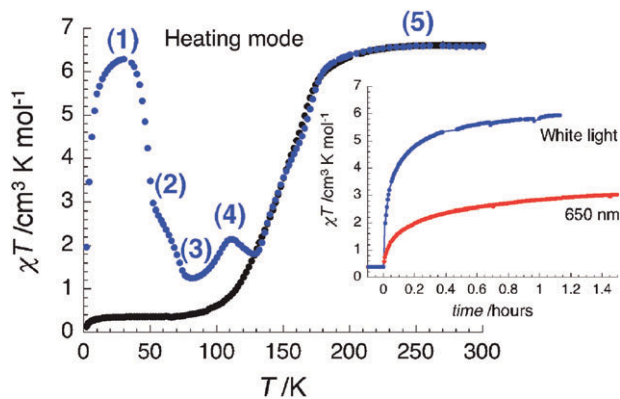


Fig. 4 Temperature dependence of the χT product after white light irradiation at 10 K for **1**. Inset: χT versus time plot at 10 K under 650 nm (30(3) mW cm^{-2}) and white (200(30) mW cm^{-2}) light irradiations at 10 K (temperature sweep rate 0.6 K/min).

Nevertheless at 110 K, this thermally induced [HS–HS] phase is still metastable and thus relaxes with a third relaxation time explaining the small drop of the χT product between 110 and 130 K, Fig. 4. Above 130 K, the expected thermal spin crossover occurs and the [HS–HS] phase is obtained above 250 K (Fig. 4, point 5).

As shown by the presented magnetic, optical and photo-magnetic properties of **1**, this fascinating new dinuclear Fe^{II} helicate displays an unusual asymmetric spin crossover behavior with a complicated relaxation of the light-induced magnetic phase. Further physical investigations (like Mössbauer spectroscopy¹⁰ and variable temperature X-ray studies) will be required to fully understand the properties of this exciting compound and form the basis of future research.

This work was financially supported by Science Foundation Ireland, the University of Canterbury, the European Network of Excellence: MAGMANet (NMP3-CT-2005-515767), the University of Bordeaux, the CNRS, the Region Aquitaine and the French Ministries of Foreign Affairs and of Research.

Notes and references

† Crystal data for **1**·2MeCN: $\text{C}_{70}\text{H}_{66}\text{Cl}_4\text{Fe}_2\text{N}_{20}\text{O}_{19}$, $M = 1744.93 \text{ g mol}^{-1}$, monoclinic, $a = 21.250(4) \text{ Å}$, $b = 10.756(2) \text{ Å}$, $c = 33.469(7) \text{ Å}$, $\beta = 90.32(3)^\circ$, $V = 7650(3) \text{ Å}^3$, $T = 150(2) \text{ K}$, $P2_1/n$ (No. 14), $Z = 4$, 82 388 reflections measured, 14 219 unique [$R(\text{int}) = 0.0513$], $wR2 = 0.1509$, $R1 = 0.0572$ (11 076 with $F \geq 4\sigma(F)$). CCDC reference number 702672.

- O. Kahn and C. J. Martinez, *Science*, 1998, **279**, 44; A. B. Gaspar, M. C. Muñoz and J. A. Real, *J. Mater. Chem.*, 2006, **16**, 2522; J. A. Real, A. B. Gaspar and M. C. Munoz, *Dalton Trans.*, 2005, 2062; K. S. Murray and C. J. Kepert, *Top. Curr. Chem.*, 2004, **233**, 195.
- O. Kahn, *Curr. Opin. Solid State Mater. Sci.*, 1996, **1**, 547; M. A. Halcrow, *Chem. Soc. Rev.*, 2008, **37**, 278; K. S. Murray, *Eur. J. Inorg. Chem.*, 2008, 3101; P. Gülich, Y. Garcia and H. A. Goodwin, *Chem. Soc. Rev.*, 2000, **29**, 419; A. Bousseksou, F. Varret, M. Goiran, K. Boukheddaden and J. P. Tuchagues, *Top. Curr. Chem.*, 2004, **233**, 65; P. Gülich and H. A. Goodwin, *Top. Curr. Chem.*, 2004, **233**, 1; Y. Garcia and P. Gülich, *Top. Curr. Chem.*, 2004, **233**, 49; A. B. Gaspar, V. Ksenofontov, M. Seredyuk and P. Gülich, *Coord. Chem. Rev.*, 2005, **249**, 2661.
- S. G. Telfer, B. Bocquet and A. F. Williams, *Inorg. Chem.*, 2001, **40**, 4818.
- F. Tuna, M. R. Lees, G. J. Clarkson and M. J. Hannon, *Chem.–Eur. J.*, 2004, **10**, 5737.
- Y. Garcia, C. M. Grunert, S. Reiman, O. van Campenhout and P. Gülich, *Eur. J. Inorg. Chem.*, 2006, 3333.
- K. Fujita, R. Kawamoto, R. Tsubouchi, Y. Sunatsuki, M. Kojima, S. Iijima and N. Matsumoto, *Chem. Lett.*, 2007, **36**, 1284.
- M. J. Hannon and L. J. Childs, *Supramol. Chem.*, 2004, **16**, 7; M. Albrecht, *Chem. Rev.*, 2001, **101**, 3457; A. Williams, *Chem.–Eur. J.*, 1997, **3**, 15; C. Piguet, G. Bernardinelli and G. Hopfgartner, *Chem. Rev.*, 1997, **97**, 2005; E. C. Constable, *Tetrahedron Lett.*, 1992, **48**, 10013; M. Albrecht and R. Frohlich, *Bull. Chem. Soc. Jpn.*, 2007, **80**, 797; P. E. Kruger, N. Martin and M. Nieuwenhuizen, *J. Chem. Soc., Dalton Trans.*, 2001, 1966; J. Keegan, P. E. Kruger, M. Nieuwenhuizen and N. Martin, *Cryst. Growth Des.*, 2002, **2**, 329; J. Keegan, P. E. Kruger, M. Nieuwenhuizen, J. O'Brien and N. Martin, *Chem. Commun.*, 2001, 2092; C. Piguet, M. Borkovec, J. Hamacek and K. Zeckert, *Coord. Chem. Rev.*, 2005, **249**, 705; B. Conerney, P. Jensen, P. E. Kruger and C. MacGloinn, *Chem. Commun.*, 2003, 1274; B. Hasenknopf, J.-M. Lehn, N. Boumediene, E. Leize and A. Van Dorsselaer, *Angew. Chem., Int. Ed.*, 1998, **37**, 3265.
- S. Goetz and P. E. Kruger, *Dalton Trans.*, 2006, 1277.
- G. Chastanet, A. B. Gaspar, J. A. Real and J. F. Létard, *Chem. Commun.*, 2001, 819; A. Bousseksou, G. Molnar, J. A. Real and K. Tanaka, *Coord. Chem. Rev.*, 2007, **251**, 1822.
- C. M. Grunert, S. Reiman, H. Spiering, J. A. Kitchen, S. Brooker and P. Gülich, *Angew. Chem., Int. Ed.*, 2008, **47**, 2997.